# FULLY AUTOMATIC RANDOM NOISE ATTENUATION USING EMPIRICAL WAVELET TRANSFORM

WEI CHEN[1,2] , HUI SONG[1,2] and XIAOYU CHUAI[3]

*[1] Key Laboratory of Exploration Technology for Oil and Gas Resources of the Ministry of Education, Yangtze University, Daxue Road 111, Caidian District, Wuhan 430100, P.R. China. chenwei_yangtze@126.com; chenwei2014@yangtzeu.edu.cn*
*[2] Hubei Cooperative Innovation Center of Unconventional Oil and Gas, Daxue Road 111, Caidian District, Wuhan 430100, P.R. China.*
*[3] Hebei Coal Research Institute, Xingtai 054000, P.R. China.*

(Received April 3, 2018; revised version accepted December 4, 2018)

ABSTRACT

Chen, W., Song, H. and Chuai, X.Y., 2019. Fully automatic random noise attenuation using empirical wavelet transform. *Journal of Seismic Exploration*, 28: 147-162.

Strong noise in seismic data seriously affects many steps in seismic data processing and imaging. While most traditional methods depend on carefully tuned input parameters by human, we are proposing an automatic noise attenuation algorithm to facilitate a fast preprocessing of massive prestack seismic data. In the proposed algorithm, the non-stationary seismic data is first adaptively decomposed into empirical components via empirical wavelet transform (EWT) according to the frequency contents in the data. Then, the first component is selected to represent the useful signals. This process can be implemented in a fully automatic way. We compare the decompositions from EWT and the empirical mode decomposition (EMD) and find that the EWT has a stronger capability in separating the useful signals and the random noise. We also test the proposed algorithm in both multi-channel synthetic and field data examples. The results demonstrate that the new adaptive method can obtain better denoising performance than the state-of-the-art methods.

KEY WORDS: random noise suppression, empirical wavelet transform, seismic signal processing, automatic processing, intrinsic mode function.

0963-0651/19/$5.00 

## INTRODUCTION

Attenuation of random seismic noise is a long-standing problem in the reflection seismology community. Because of the crucial benefits of removing random noise to many seismic processing and imaging tasks, dozens of methods to attenuate seismic noise, also known as denoise, have been investigated in the literature in the past decades (Chen and Fomel, 2015; Qu et al., 2015; Gan et al., 2016e; Zu et al., 2017c; Yang et al., 2018; Li et al., 2016a,b; Qu et al., 2016; Chen, 2018a).

The simpest denoising method is by stacking the seismic data along the offset direction (Yang et al., 2015; Zu et al., 2016b). By stacking the useful signals from multiple traces and multiple directions (e.g., offset and midpoint), the signal is enhanced while influence of noise is mitigated. Prediction based methods utilize the predictable property of useful signals to construct prediction filterers to enhance signals and reject noise, for example, t-x predictive filtering (Abma and Claerbout, 1995), f-x deconvolution (Canales, 1984), the polynomial fitting based approach (Liu et al., 2011; Chen et al., 2018), non-stationary predictive filtering (Liu and Chen, 2013). Different types of median filters can be used to remove spike-like noise in seismic data (Gan et al., 2016d; Bai and Wu, 2017; Zu et al., 2017a,b; Zhao et al., 2018; Xie et al., 2018).

Sparse transform based approaches first transform seismic data to a sparse domain, then apply soft thresholding to the coefficients, finally transform the sparse coefficients back to the time-space domain (Chen et al., 2016a). Widely used sparse transforms are Fourier transform (Zhong et al., 2016), curvelet transform (Candès et al., 2006; Neelamani et al., 2008; Liu et al., 2016c; Zu et al., 2016a), seislet transform (Fomel and Liu, 2010; Chen et al., 2014; Gan et al., 2015b, 2016c; Liu et al., 2016d; Wu et al., 2016; Bai and Wu, 2018), Radon transform (Xue et al., 2016b, 2017; Chen, 2018b), and different types of wavelet transforms (e.g., physical, synchrosqueezing, etc) (Donoho and Johnstone, 1994; Zhang and Ulrych, 2003; Gao et al., 2006; Liu et al., 2016e,b). A recently popular transform is based on the machine learning engine to train adaptive transform basis in order to better deal with the complexity in various types of seismic data, which is called the dictionary learning based sparse transform (Chen, 2017; Siahsar et al., 2017; Wu and Bai, 2018).

Decomposition based approaches decompose the noisy seismic data into different components and then select the principal components to represent the useful signals. Empirical mode decomposition (EMD) and its variations (Chen and Ma, 2014; Chen, 2016; Gan et al., 2016a,b; Chen and Fomel, 2018), variational mode decomposition (Liu et al., 2016a, 2017), singular value decomposition based approaches (Bekara and van der Baan, 2007; Gan et al., 2015a; Chen et al., 2016b; Xue et al., 2016a; Zhang et al.,

2016; Wang et al., 2017; Zhou et al., 2017; Chen et al., 2017; Zhou et al., 2018; Bai et al., 2018), regularized non-stationary decomposition based approaches (Wu et al., 2018; Chen, 2018c) are frequently used to extract the useful components in multi-dimensional seismic data in the literature.

Although there are many existing denoising approaches, no approaches are completely automatic so far. The traditional methods reply on more or less input parameters that requires heuristic knowledge and thus are not convenient to apply. In this paper, we propose a fully automatic denoising algorithm based on the empirical wavelet transform (EWT) (Gilles, 2013). The EWT method can also adaptively decompose a signal containing many frequency components into corresponding frequency signals as EMD or EEMD does, but the modes generated from the raw signal can be reasonably interpreted. It is worth mentioning that the EWT has been applied in time-frequency analysis in many fields, including the seismic data analysis field (Liu et al., 2016b). However, it has never been applied to denoise seismic data so far. Here, we are reporting a successful application of the adaptive signal decomposition technique to automatic seismic noise attenuation. We will show in details how the method works and how the denoising performance looks like using several realistic examples.

## METHOD

We denote the analyzed signal as s (t). In the time domain, wavelet sets $\{\psi_{i,j}\}$ are defined by mother wavelet function $\psi_{u,v}$ with mean value zero, scale factor v ($v > 0$) and shift factor u ($u > 0$).

We consider a normalized Fourier axis with period $2\pi$, and make discussions in consideration of Fourier frequency domain as $\omega \in [0, \pi]$ in order to satisfy the Shannon theorem.

Next, we disperse the Fourier frequency domain $[0, \pi]$ into N continuous subintervals, so we get N + 1 discontinuity points and denote the nth one as $\omega_{n+1}$, the first one as $\omega_0 = 0$ and the last one as $\omega_N = \pi$. Then we can get the nth subinterval as $d_n = [\omega_{n-1},\omega_n]$. It is clear that $\cup^N_{n=1} d_n = [0,\pi]$. If we center on discontinuity point $\omega_n$, a transitional zone denoted as $T_n$ whose width is $2\tau_n$ can be defined.

Empirical wavelet is defined as a band-pass filter on the domain $d_n$. In addition, for the half of the width of the transition zone $\tau_n$, we generally have $\tau_n = \gamma\omega_n$, and $0 < \gamma < 1$. Similar to the structure strategy of Littlewood-Paley wavelet and Meyer wavelet (Gilles, 2013), for $\forall\, n > 0$, we can define the empirical scale function as:

$$\hat{\phi}_n(\omega)\begin{cases} 1, & |\omega| \le (1-\gamma)\omega_n \\ cos\left[\frac{\pi}{2}\beta\left(\frac{1}{2\gamma\omega_n}(|\omega| - (1-\gamma)\omega_n)\right)\right], & \\ \quad (1-\gamma)\omega_n \le |\omega| \le (1+\gamma)\omega_n & \\ 0, & \text{else} \end{cases} \tag{1}$$

and empirical wavelet as:

$$\hat{\psi}_n(\omega)\begin{cases} 1, & (1+\gamma)\omega_n \le |w| \le (1-\gamma)\,\omega_{n+1} \\ cos\left[\frac{\pi}{2}\beta\left(\frac{1}{2\gamma\omega_{n+1}}(|\omega| - (1-\gamma)\,\omega_{n+1})\right)\right], & \\ \quad (1-\gamma)\,\omega_{n+1} \le |\omega| \le (1+\gamma)\omega_{n+1} & \\ sin\left[\frac{\pi}{2}\beta\left(\frac{1}{2\gamma\omega_n}(|\omega| - (1-\gamma)\,\omega_n)\right)\right], & \\ \quad (1-\gamma)\,\omega_n \le |\omega| \le (1+\gamma)\,\omega_n & \\ 0, & \text{else} \end{cases} \tag{2}$$

In the above two equations, β (x) is 0 or 1, and generally we have

$$\beta(x) = x^4\left(35 - 84x + 70x^2 - 20x^3\right) \quad . \tag{3}$$

How to divide the Fourier spectrum is of vital importance in EWT, which is directly related to the adaptivity of the decomposition of the original signal. Here we imitate the classical wavelet transform theory to define the EWT, so the detailed coefficients are defined by the inner product of empirical wavelet and original signal:

$$W_s{}^{\varepsilon}(n,t) = \langle s, \psi_n \rangle = \int s(\tau)\,\overline{\psi_n(\tau - t)}d\tau \quad , \tag{4}$$

$W_S{}^{\varepsilon}(n,t)$ in eq. (4) can also be expressed as $c_n(t)$ and the summation of $c_n(t)$ reconstructs the original signal s(t). In an EMD-like format, we have

$$s(t) = \sum_{i=1}^{N} c_n(t) \quad , \tag{5}$$

where $c_n(t)$ denotes the nth component and is also called intrinsic mode function (IMF). N denotes the number of components. Different component after EWT decomposition usually correspond to different frequency bands. The first component, i.e., $c_1(t)$ is usually corresponding to the most distinct/dominant frequency band, which indicates the frequency band of the reflection signals.

The beauty of the EWT method is that the decomposition process is fully automatic. Although EMD has a similar advantage of being adaptive, it is remained as empirical. Because of the lack of mathematical support, the modes in EMD are not flexibly controlled.

An example of the EWT decomposition is shown in Figs. 1-4. Fig. 1 shows a single-trace synthetic example. In Fig. 1, (a) denotes a clean seismic trace and (b) denotes a noisy seismic trace, with a signal-to-noise ratio (SNR) equal to 0.32 dB. The definition of SNR is defined as

$$SNR = 10\log_{10}\frac{\|\mathbf{d}_{clean}\|_2^2}{\|\mathbf{d}_{denoised}-\mathbf{d}\|_2^2}\quad , \tag{6}$$

where $d_{clean}$ denotes the exact solution, i.e., the clean data, and $d_{denoised}$ denotes the denoised data.

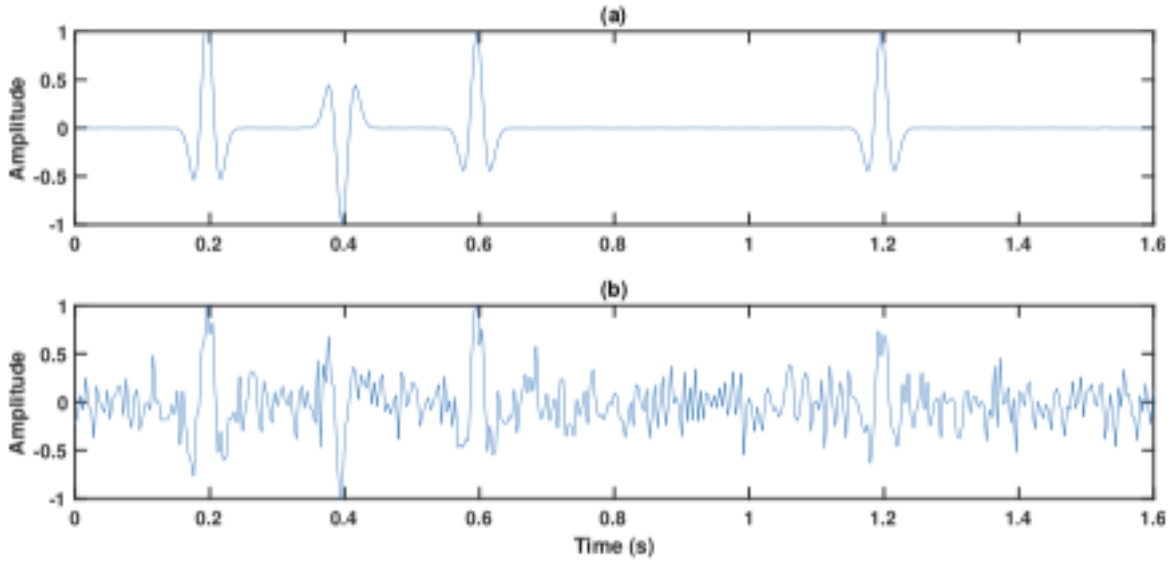


Fig. 1. Single-trace example. (a) Clean seismic trace. (b) Noisy seismic trace.

Fig. 2 shows the decomposed results using EWT. (a)-(e) denote the first to fifth components, respectively. It is clear that first component mainly represents the useful signals. Fig. 3 shows the decomposed results using EMD. (a)-(h) denote the first to eighth components. It is obvious that most decomposed components are irregular and do not show clear morphological structure of the useful signals. In EMD method, in order to preserve sufficient useful signals, we usually remove only the first component, which stands for the high-frequency oscillating information. Fig. 4 provides a comparison between two methods. The clean data is also shown as a reference. It is clear that the denoised data (shown in c) is much smoother and cleaner than that from the EMD method (shown in e). It is encouraging that the EWT method recovers the Ricker waveform very well due to the use of wavelet basis function. The SNRs of the denoised results using EWT and EMD are 5.32 dB and 4.13 dB, respectively.

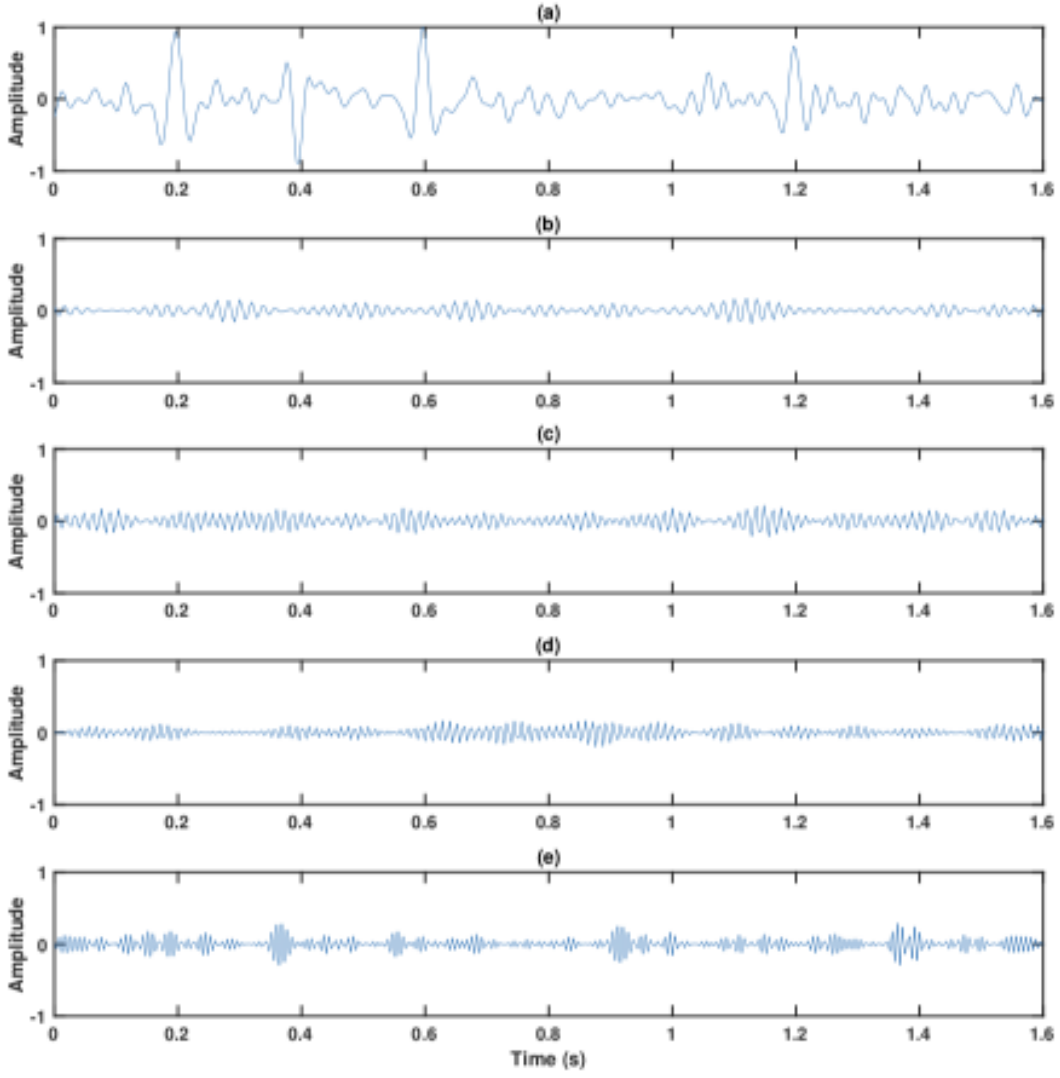


Fig. 2. Decomposed results using EWT. (a)-(e): First to fifth components.

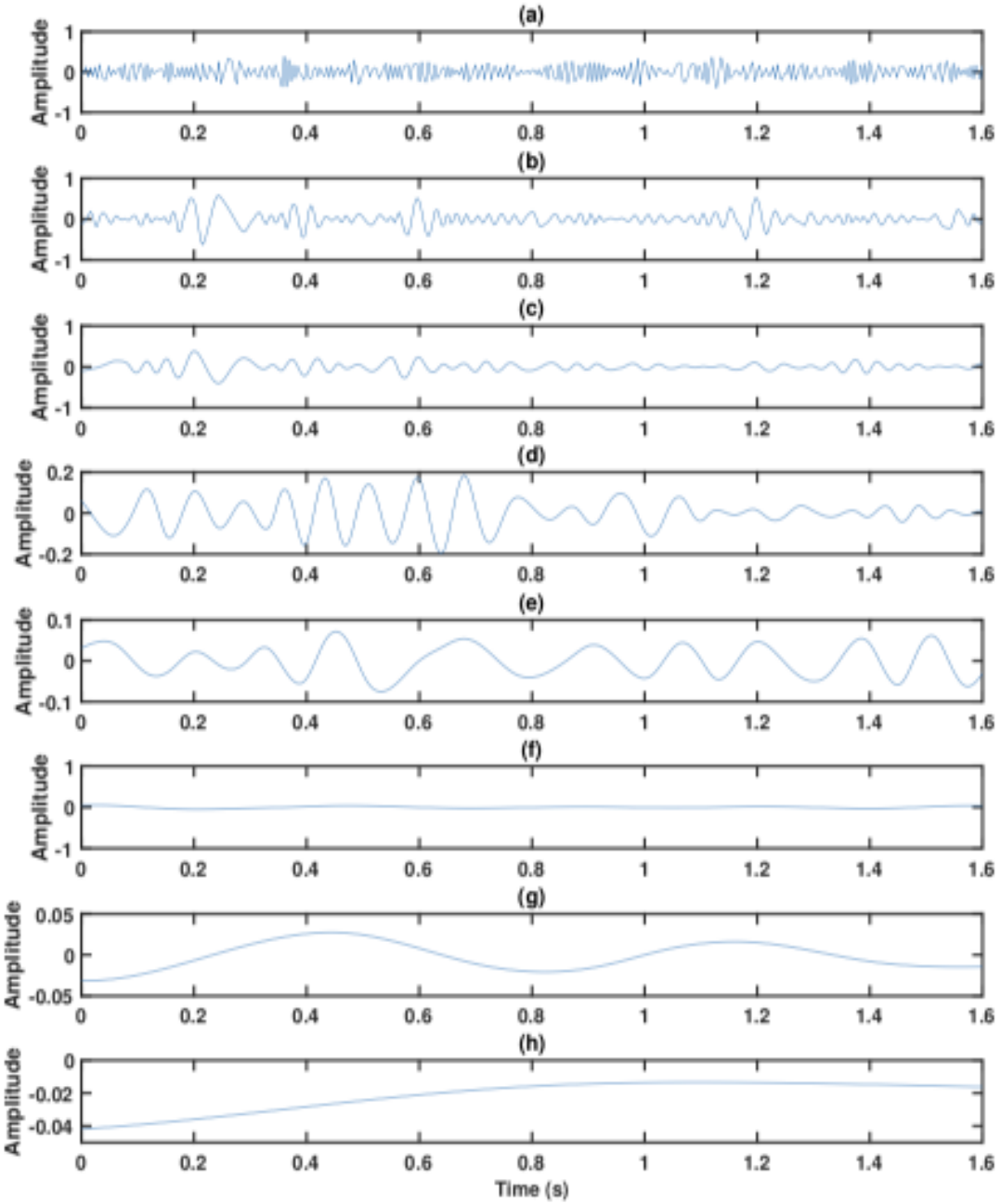


Fig. 3. Decomposed results using EMD. (a)- (h): First to eighth components.

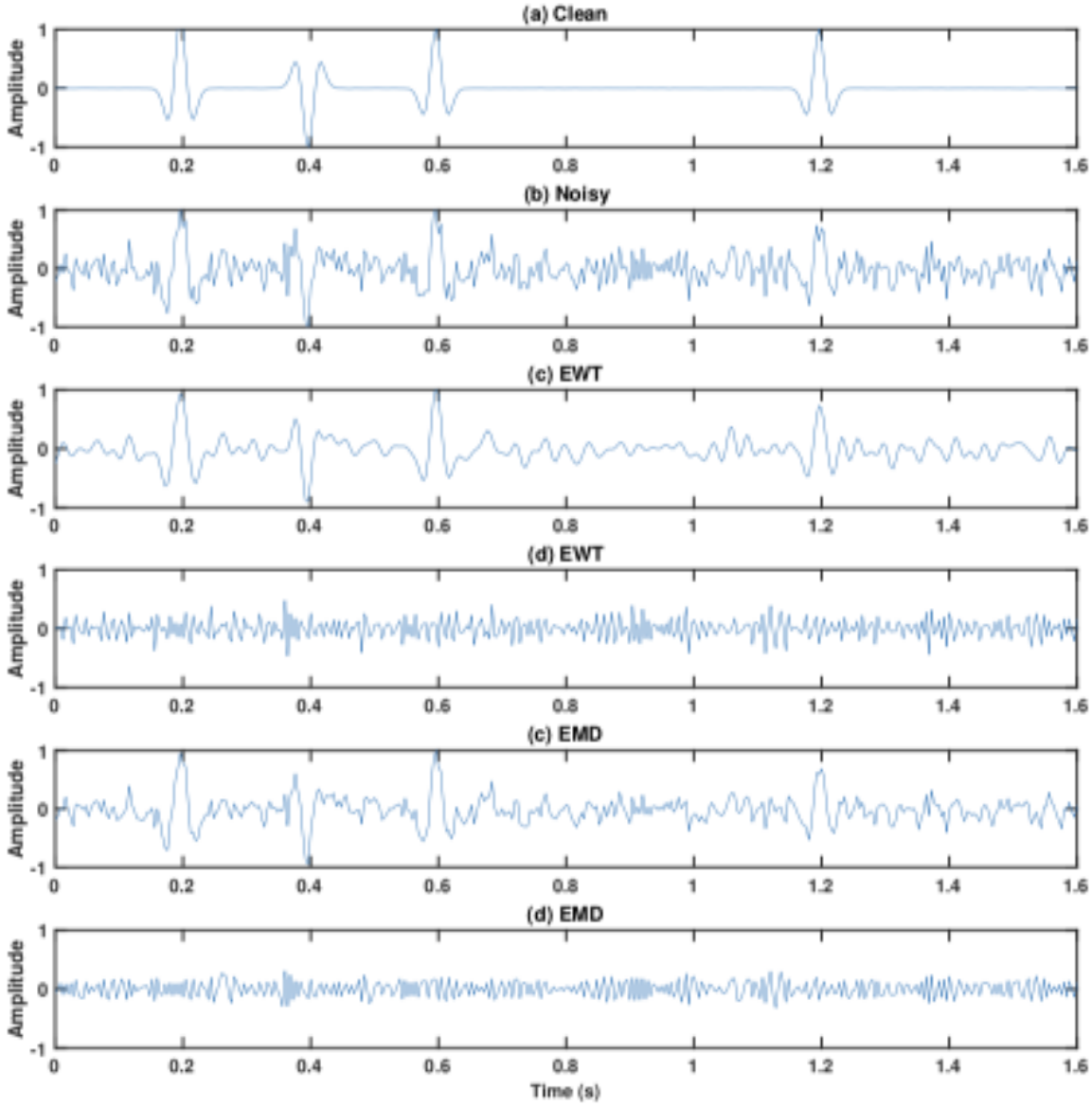


Fig. 4. Comparison of signal-and-noise separation performance. (a) Clean data. (b) Noisy data. (c) Denoised data using EWT. (d) Noise from the EWT method. (e) Denoised data using EMD. (f) Noise from the EMD method.

## EXAMPLES

In this section, we mainly focus on investigating the performance of the proposed method when applied to multi-channel seismic data and comparing the performance from the pro- posed method with some state-of-the-art methods. Fig. 5 shows the synthetic example. The synthetic data is very realistic, because it contains several typical morphological

structures that are common in seismic data, e.g., the crossing and curving events, faults, and discontinuities. Fig. 6 shows a comparison of denoised data using four different methods. Fig. 6a shows the result from the FX method. For the FX method, we use a prediction filter of 6 points length. Fig. 6b shows the result from the SSA method. To deal with the complicated structure, we use a rank equal to 10. For the proposed method, as mentioned previously, we do not specify any parameters. From the denoised results, it is straightforward to conclude that both FX and SSA methods damage a lot of the edges. It is clear that the discontinuities in Fig. 5 are smeared a lot. Since FX and SSA methods are both based on the spatial coherency of the seismic events, they will inevitably make the denoised data spatially smoothed. However, the proposed method seems to obtain a successful preservation of the edges.

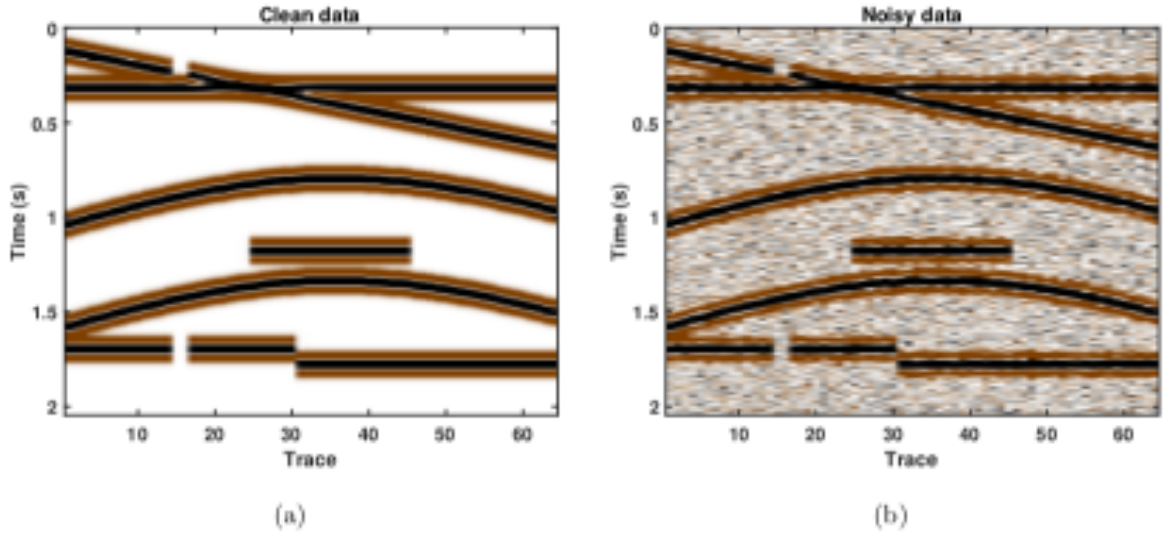


Fig. 5. Synthetic example. (a) Clean data. (b) Noisy data.

To compare the denoising performance, it is useful to compare the removed noise. The removed noise is calculated by subtracting the denoised data (each subfigure in Fig. 6) from the noisy data (in Fig. 5b). Ideally, the removed noise should only contain random noise. If there is spatially coherent energy in the removed noise, it indicates that the denoising method damages some useful energy. We show the removed noise corresponding to four different methods in Fig. 7. Fig. 7a corresponds to the FX method, which contains significant coherent energy. Fig. 7b shows the noise from the SSA method, which also contains a lot of coherent energy, especially those edge positions. Fig. 7c, however, does not contain any coherent energy. From this comparison, we conclude that only the proposed method among

the four aforementioned methods can preserve all the useful signals. To make a quantitative comparison, we calculate the SNRs corresponding to the FX, SSA, and the proposed methods as 14.87 dB, 13.36 dB, and 15.37 dB, respectively. Note that the SNR of the noisy data (shown in Fig. 5b) is 7.49 dB. We find that the proposed method obtains the largest SNR improvement. It is also worth mentioning that both FX and SSA methods are tuned carefully to ensure the best performance to be presented.

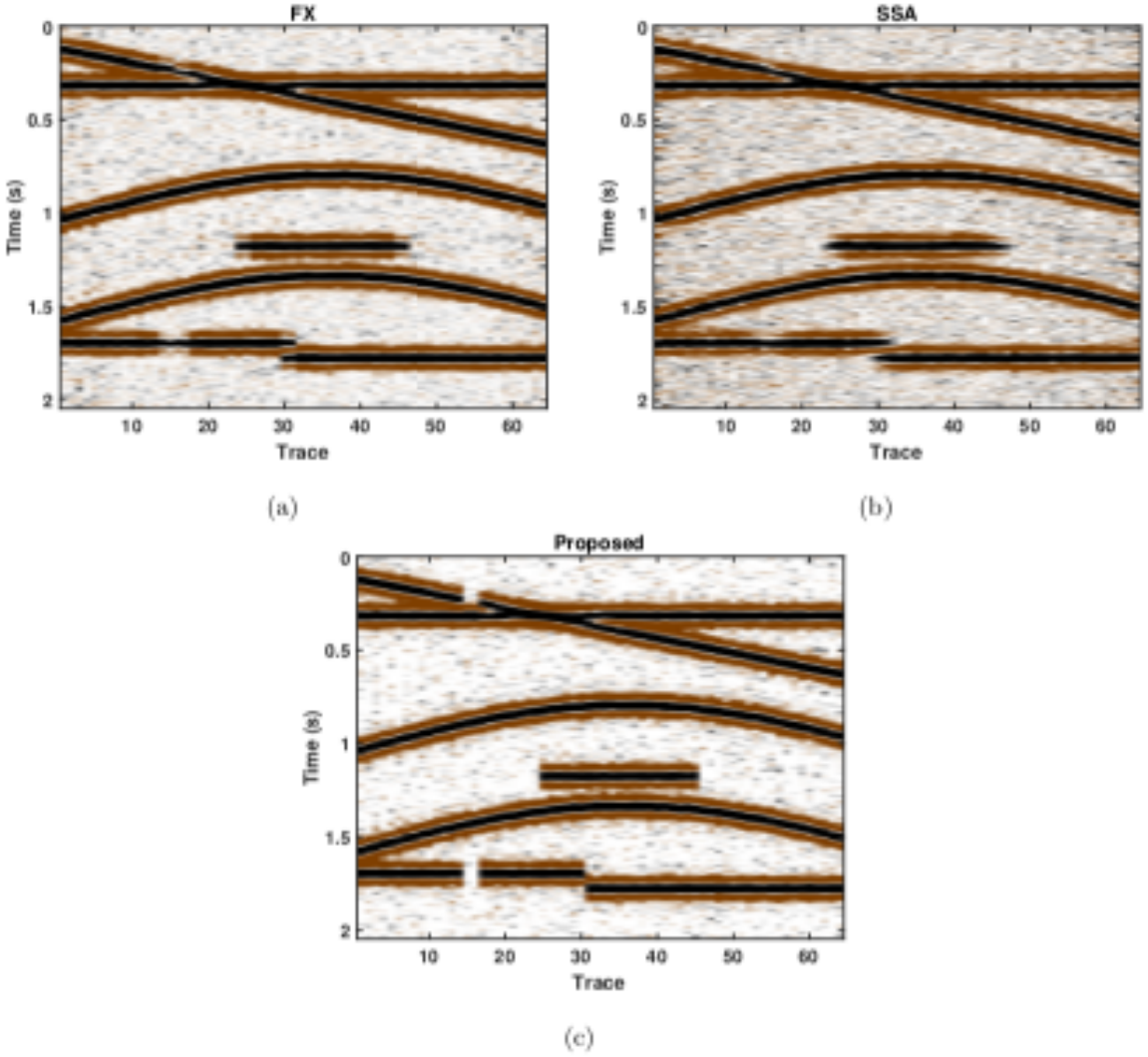


Fig. 6. Comparison of the denoised data for the synthetic example. (a) Denoised data using FX method. (b) Denoised data using SSA method. (c) Denoised data using the proposed method.

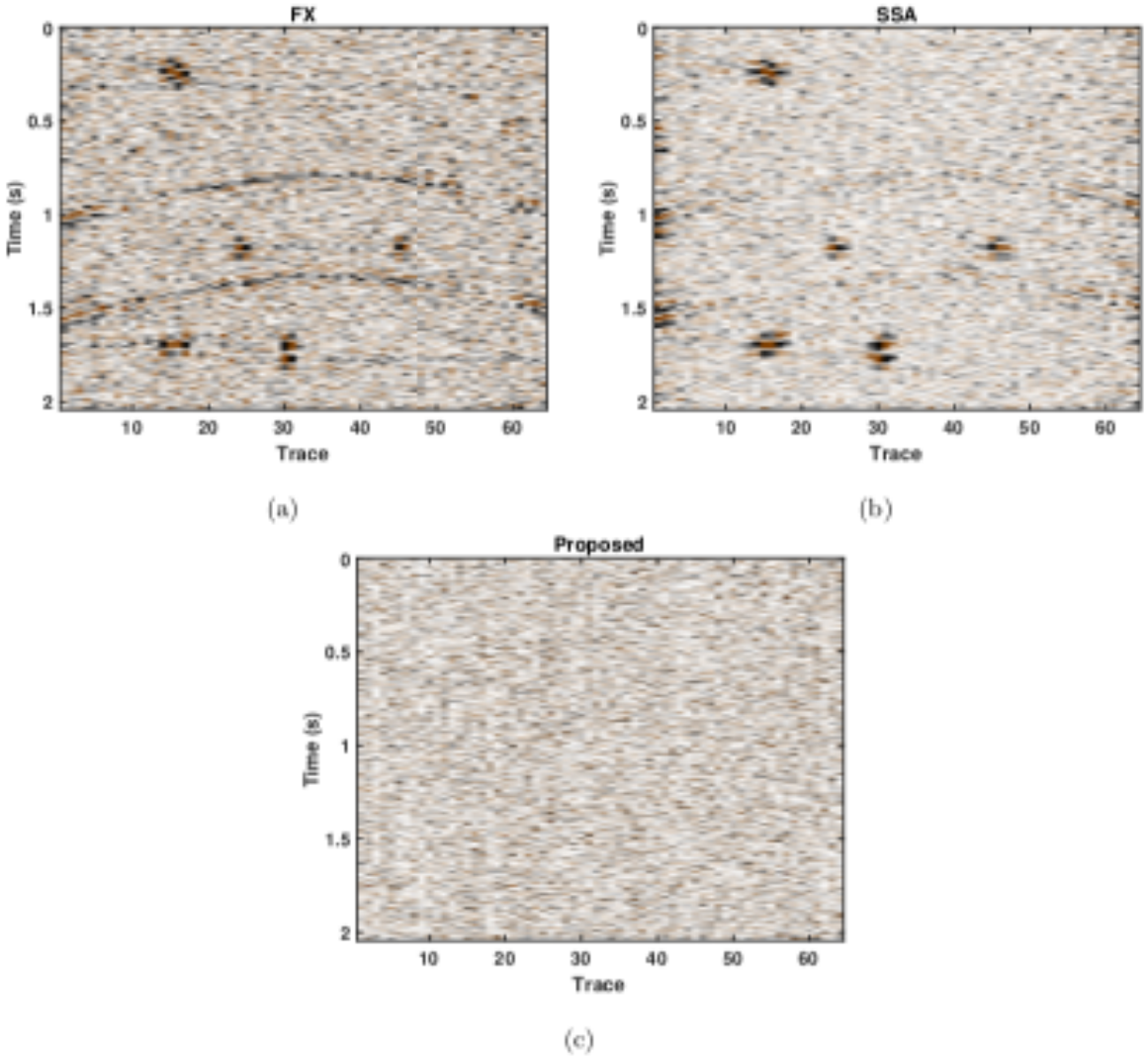


Fig. 7. Comparison of the removed noise for the synthetic example. (a) Removed noise using FX method. (b) Removed noise using SSA method. (c) Removed noise using the proposed method.

To further examine the performance, our proposed method is applied to a post-stack field seismic data set, which consists of 219 traces and 1251 samples with a sample interval of 4 ms, as shown in Fig. 8. The data set mainly includes discontinuous events, nonstationary events, and faults. In other words, the non-linear and non-stationary signals in this data set are widespread. From Fig. 8, it is obvious that the useful signal is blurred by noise. The signal is no longer mapped to a superposition of simple harmonics but rather a superposition of non-linear and non-stationary ones. The performance of this example is shown in Fig. 8. In Fig. 8, the left panel denotes the raw field data, the middle panel denotes the denoised data using

the proposed method, the right panel denotes the removed noise. Note that for processing such complicated field data, it is exciting that we do not specify any parameters for the proposed method. Thus, the automatic benefit is the best advantage of the proposed method, which is exceptionally important when dealing with massive seismic data.

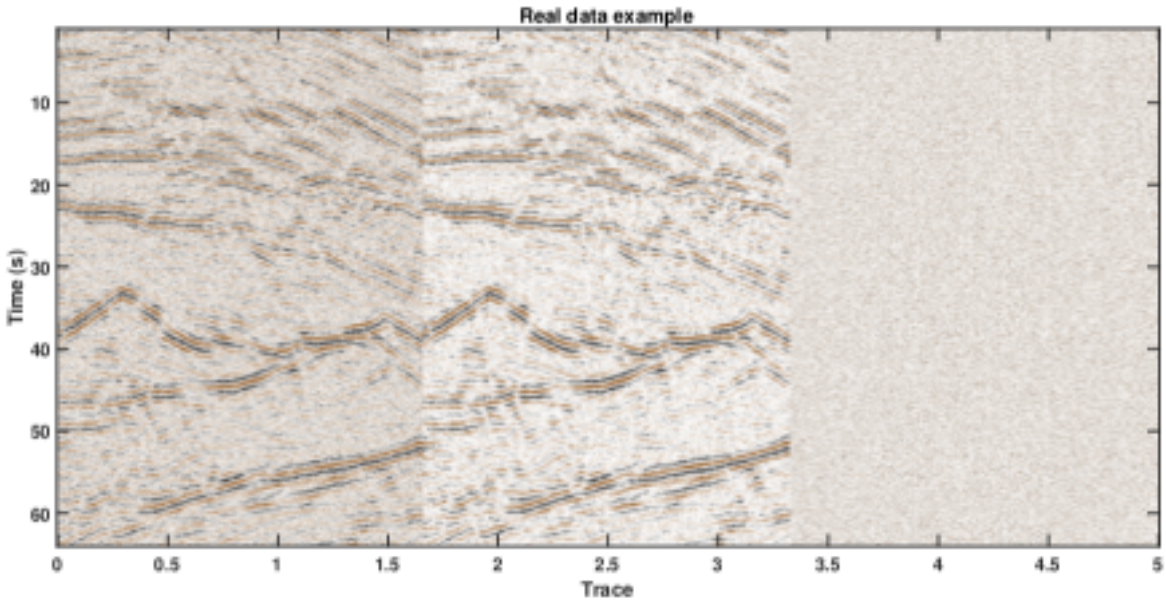


Fig. 8. Field data example. Left: noisy data. Middle: denoised data. Right: removed noise.

## CONCLUSIONS

We have introduced a simple and adaptive denoising algorithm based on the empirical wavelet transform (EWT). The EWT has a stronger mathematical background than the empirical mode decomposition (EMD) method and also has a better signal-and-noise separability. In the proposed method, single-trace seismic data is first decomposed into different modes. Then, the first decomposed component is selected to represent the useful reflection signals. The method is free of input parameters and thus is very easy to apply. We demonstrate through both synthetic and field data examples, that the proposed method can preserve spatial edges and does not damage useful signals when applied to denoise multi-channel seismic data.

## ACKNOWLEDGEMENTS

This work is supported by the National Natural Science Foundation of China (Grant No. 41804140) and the Open Fund of Key Laboratory of Exploration Technologies for Oil and Gas Resources (Yangtze University), Ministry of Education (Grant No. PI2018-02) .

## REFERENCES

Abma, R. and Claerbout, J.,1995. Lateral prediction for noise attenuation by t−x and f−x techniques. Geophysics, 60: 1887-1896.

Bai, M. and Wu, J., 2017,. Efficient deblending using median filtering without correct normal moveout - with comparison on migrated images. J. Seismic Explor., 26: 455-479.

Bai, M. and Wu, J., 2018. Seismic deconvolution using iteartive transform-domain sparse inversion. J. Seismic Explor., 27: 103-116.

Bai, M., Wu, J., Xie, J. and Zhang, D., 2018. Least-squares reverse time migration of blended data with low-rank constraint along structural direction. J. Seismic Explor., 27: 29-48.

Bekara, M. and van der Baan, M., 2007. Local singular value decomposition for signal enhancement of seismic data. Geophysics, 72: V59-V65.

Canales, L., 1984. Random noise reduction. Expanded Abstr, 54th Ann. Internat. SEG Mtg., Atlanta: 525-527.

Candès, E.J., Demanet, L., Donoho, D.L. and Ying, L., 2006. Fast discrete curvelet transforms. SIAM Multisc. Model. Simulat., 5: 861-899.

Chen, Y., 2016. Dip-separated structural filtering using seislet thresholding and adaptive empirical mode decomposition based dip filter. Geophys. J. Internat., 206: 457-469.

Chen, Y., 2017. Fast dictionary learning for noise attenuation of multidimensional seismic data. Geophys. J. Internat., 209: 21–31.

Chen, Y., 2018a. Automatic microseismic event picking via unsupervised machine learning. Geophys. J. Internat., 212: 88-102.

Chen, Y., 2018b. Automatic velocity analysis using high-resolution hyperbolic Radon transform. Geophysis, 83(4): A53-A57.

Chen, Y., 2018c. Non-stationary least-squares complex decomposition for microseismic noise attenuation. Geophys. J. Internat., 213: 1572-1585.

Chen, Y., Chen, H., Xiang, K. and Chen, X., 2017. Preserving the discontinuities in least-squares reverse time migration of simultaneous-source data. Geophysics, 82(3). doi: 10.1190/GEO2016–0456.1.

Chen, Y., and Fomel, S., 2015. Random noise attenuation using local signal-and-noise orthogonalization. Geophysics, 80: WD1–WD9.

Chen, Y., 2018. EMD-seislet transform. Geophysics, 83(1): A27-A32.

Chen, Y., Fomel, S. and Hu, J., 2014. Iterative deblending of simultaneous-source seismic data using seislet-domain shaping regularization. Geophysics, 79(5): V179-V189.

Chen, Y., Huang, W., Zhou, Y., Liu, W. and Zhang, D., 2018. Plane-wave orthogonal polynomial transform for amplitude-preserving noise attenuation. Geophys. J. Internat., 214: 2207–2223.

Chen, Y. and Ma, J., 2014. Random noise attenuation by f-x empirical mode decomposition predictive filtering. Geophysics, 79: V81–V91.

Chen, Y., Ma, J. and Fomel, S., 2016a. Double-sparsity dictionary for seismic noise attenuation. Geophysics, 81: V17–V30.

Chen, Y., Zhang, D., Jin, Z., Chen, X., Zu, S., Huang, W. and Gan, S., 2016b. Simultaneous denoising and reconstruction of 5D seismic data via damped rank-reduction method. Geophys. J. Internat., 206: 1695-1717.

Donoho, D.L. and Johnstone, I.M., 1994. Ideal spatial adaptation by wavelet shrinkage: Biometrika, 81: 425-455.

Fomel, S. and Liu, Y., 2010. Seislet transform and seislet frame. Geophysics, 75: V25-V38.

Gan, S., Chen, Y., Wang, S., Chen, X., Huang, W. and Chen, H., 2016a. Compressive sensing for seismic data reconstruction using a fast projection onto convex sets algorithm based on the seislet transform. J. Appl. Geophys., 130: 194-208.

Gan, S., Chen, Y., Zu, S., Qu, S. and Zhong, W., 2015a. Structure-oriented singular value decomposition for signal enhancement of seismic data. J. Geophys. Engineer., 12: 262-272.

Gan, S., Wang, S., Chen, Y., Chen, J., Zhong, W. and Zhang, C., 2016b. Improved random noise attenuation using f-x empirical mode decomposition and local similarity. Appl. Geophys., 13: 127-134.

Gan, S., Wang, S., Chen, Y. and Chen, X., 2016c. Simultaneous-source separation using iterative seislet-frame thresholding. IEEE Geosci. Remote Sens. Lett., 13: 197-201.

Gan, S., Wang, S., Chen, Y., Chen, X. and Xiang, K., 2016d. Separation of simultaneous sources using a structural-oriented median filter in the flattened dimension. Comput. Geosci., 86: 46-54.

Gan, S., Wang, S., Chen, Y., Qu, S. and Zu, S., 2016e. Velocity analysis of simultaneous-source data using high-resolution semblance-coping with the strong noise. Geophys. J. Internat., 204: 768-779.

Gan, S., Wang, S., Chen, Y., Zhang, Y. and Jin, Z., 2015b. Dealiased seismic data interpolation using seislet transform with low-frequency constraint. IEEE Geosci. Remote Sens. Lett., 12: 2150-2154.

Gao, J., Mao, J., Chen, W. and Zheng, Q., 2006. On the denoising method of prestack seismic data in wavelet domain. Chin. J. Geophys., 49: 1155-1163.

Gilles, J., 2013. Empirical wavelet transform. IEEE Transact. Sign. Process., 61: 3999-4010.

Li, H., Wang, R., Cao, S., Chen, Y. and W. Huang, W., 2016a. A method for low-frequency noise suppression based on mathematical morphology in microseismic monitoring. Geophysics, 81(3), V159-V167.

Li, H., Wang, R., Cao, S., Chen, Y., Tian, N. and Chen, X., 2016b. Weak signal detection using multiscale morphology in microseismic monitoring. J. Appl. Geophys., 133: 39-49.

Liu, G. and Chen, X., 2013. Noncausal f-x-y regularized nonstationary prediction filtering for random noise attenuation on 3D seismic data. J. Appl. Geophys., 93: 60-66.

Liu, G., Chen, X., Du, J. and Song, J., 2011. Seismic noise attenuation using nonstationary polynomial fitting. Appl. Geophys., 8: 18-26.

Liu, W., Cao, S. and Chen, Y., 2016a. Applications of variational mode decomposition in seismic time-frequency analysis. Geophysics, 81(5): V365-V378.

Liu, W., Cao, S. and Chen, Y., 2016b. Seismic time-frequency analysis via empirical wavelet transform. IEEE Geosci. Remote Sens. Lett., 13: 28-32.

Liu, W., Cao, S., Chen, Y. and Zu, S., 2016c. An effective approach to attenuate random noise based on compressive sensing and curvelet transform. J. Geophys. Engineer., 13: 135-145.

Liu, W., Cao, S., Gan, S., Chen, Y., Zu, S. and Jin, Z., 2016d. One-step slope estimation or dealiased seismic data reconstruction via iterative seislet thresholding. IEEE Geosci. Remote Sens. Lett., 13: 1462-1466.

Liu, W., Cao, S., Liu, Y. and Chen, Y., 2016e. Synchrosqueezing transform and its applications in seismic data analysis. J. Seismic Explor., 25: 27-44.

Liu, W., Cao, S., Wang, Z., Kong, X. and Chen, Y., 2017. Spectral decomposition for hydrocarbon detection based on YMD and Teager-Kaiser energy. IEEE Geosci. Remote Sens. Lett., 14: 539-543.

Neelamani, R., Baumstein, A., Gillard, D., Hadidi, M. and Soroka, W., 2008. Coherent and random noise attenuation using the curvelet transform. The Leading Edge, 27: 240-248.

Qu, S., Zhou, H., Chen, Y., Yu, S., Zhang, H., Yuan, J., Yang, Y. and Qin, M., 2015. An effective method for reducing harmonic distortion in correlated vibroseis data. J. Appl. Geophys., 115: 120-128.

Qu, S., Zhou, H., Liu, R., Chen, Y., Zu, S., Yu, S., Yuan, J. and Yang, Y., 2016. Deblending of simultaneous-source seismic data using fast iterative shrinkage-thresholding algorithm with firm-thresholding. Acta Geophys., 64: 1064-1092.

Siahsar, M.A.N., Abolghasemi, V. and Chen, Y., 2017. Simultaneous denoising and interpolation of 2D seismic data using data-driven non-negative dictionary learning. Sign. Process., 141: 309-321.

Wang, Y., Zhou, H., Zu, S., Mao, W. and Chen, Y., 2017. Three-operator proximal splitting scheme for 3D seismic data reconstruction. IEEE Geosci. Remote Sens. Lett., 14: 1830-1834.

Wu, G., Fomel, S. and Chen, Y., 2018. Data-driven time-frequency analysis of seismic data using non-stationary prony method. Geophys. Prosp., 66: 85-97.

Wu, J. and Bai, M., 2018. Incoherent dictionary learning for reducing crosstalk noise in least-squares reverse time migration. Comput. Geosci., 114: 11-21.

Wu, J., Wang, R., Chen, Y., Zhang, Y., Gan, S. and Zhou, C., 2016. Multiples attenuation using shaping regularization with seislet domain sparsity constraint. J. Seismic Explor., 25: 1-9.

Xie, J., Di, B., Schmitt, D., Wei, J. and Chen, Y., 2018. Estimation of $\delta$ and $c_{13}$ of organic-rich shale from laser ultrasonic technique (LUT) measurement. Geophysics, 83(4): C137-C152.

Xue, Y., Chang, F., Zhang, D. and Chen, Y., 2016a. Simultaneous sources separation via an iterative rank-increasing method. IEEE Geosci. Remote Sens. Lett., 13: 1915-1919.

Xue, Y., Man, M., Zu, S., Chang, F. and Chen, Y., 2017. Amplitude-preserving iterative deblending of simultaneous source seismic data using high-order radon transform. J. Appl. Geophys., 139: 79-90.

Xue, Y., Yang, J., Ma, J. and Chen, Y., 2016b. Amplitude-preserving nonlinear adaptive multiple attenuation using the high-order sparse radon transform. J. Geophys. Engineer., 13: 207-219.

Yang, W., Wang, R., Wu, J., Chen, Y., Gan, S. and Zhong, W., 2015. An efficient and effective common reflection surface stacking approach using local similarity and plane-wave flattening. J. Appl. Geophys., 117: 67-72.

Yang, Y., Li, D., Tong, T., Zhang, D., Zhou, Y. and Chen, Y., 2018. Denoising controlled-source electromagnetic data using least-squares inversion. Geophysics, 83(4): E229-E244.

Zhang, D., Chen, Y., Huang, W. and S. Gan, S., 2016. Multi-step damped multichannel singular spectrum analysis for simultaneous reconstruction and denoising of 3D seismic data. J. Geophys. Engineer., 13: 704-720.

Zhang, R. and Ulrych, T., 2003. Physical wavelet frame denoising. Geophysics, 68: 225-231.

Zhao, Q., Du, Q., Gong, X. and Chen, Y., 2018. Signal-preserving erratic noise attenuation via iterative robust sparsity-promoting filter. IEEE Transact. Geosci. Remote Sens., 56: 1558-1564.

Zhong, W., Chen, Y., Gan, S. and Yuan, J., 2016. $L_{1/2}$ norm regularization for 3D seismic data interpolation. J. Seismic Explor., 25: 257-268.

Zhou, Y., Li, S., Zhang, D. and Chen, Y., 2018. Seismic noise attenuation using an online subspace tracking algorithm. Geophys. J. Internat., 212: 1072-1097.

Zhou, Y., Shi, C., Chen, H., Xie, J., Wu, G. and Chen, Y., 2017. Spike-like blending noise attenuation using structural low-rank decomposition. IEEE Geosci. Remote Sens. Lett., 14: 1633-1637.

Zu, S., Zhou, H., Chen, H., Zheng, H. and Chen, Y., 2017a. Two field trials for deblending of simultaneous source surveys: why we failed and why we succeeded? J. Appl. Geophys., 143: 182-194.

Zu, S., Zhou, H., Chen, Y., Qu, S., Zou, X., Chen, H. and Liu, R., 2016a. A periodically varying code for improving deblending of simultaneous sources in marine acquisition. Geophysics, 81: V213-V225.

Zu, S., Zhou, H., Chen, Y., Pan, X., Gan, S. and Zhang, D., 2016b. Interpolating big gaps using inversion with slope constraint. IEEE Geosci. Remote Sens. Lett., 13: 1369-1373.

Zu, S., Zhou, H., Li, Q., Chen, H., Zhang, Q., Mao, W. and Chen, Y., 2017b. Shot-domain deblending using least-squares inversion. Geophysics, 82(4): V241-V256.

Zu, S., Zhou, H., Mao, W., Zhang, D., Li, C., Pan, X. and Chen, Y., 2017c. Iterative deblending of simultaneous-source data using a coherency-pass shaping operator. Geophys. J. Internat., 211: 541-557.